Genetic architecture and lifetime dynamics of inbreeding depression in a wild mammal

Authors names and addresses:

Stoffel, M.A.[1*], Johnston, S.E.[1], Pilkington, J.G.[1], Pemberton, J.M[1]

[1]Institute of Evolutionary Biology, School of Biological Sciences, University of Edinburgh, Edinburgh, EH9 3FL, United Kingdom

* Corresponding author:

Martin A. Stoffel

Postal address: Institute of Evolutionary Biology, University of Edinburgh, Edinburgh, EH9 3FL, UK

E-mail: martin.stoffel@ed.ac.uk

Abstract

Inbreeding depression is a phenomenon of long-standing importance, but we know surprisingly little about its genetic architecture, precise effects and life-history dynamics in wild populations. Here, we combined 417K imputed SNP genotypes for 5952 wild Soay sheep with detailed long-term life-history data to explore inbreeding depression on a key fitness component, annual survival. Inbreeding manifests in long runs of homozygosity (ROH) and these are abundant in Soay sheep, covering on average 24% of the autosomal genome and up to 50% in the most inbred individuals. The ROH landscape is shaped by recombination rate variation and differs widely across the genome, including islands where up to 87% of the population have an ROH and deserts where the ROH prevalence is as low as 4%. We next quantified individual inbreeding as the proportion of the autosomal genome in ROH (F_{ROH}) and estimated its effect on annual survival. The consequences of inbreeding are severe; a 10% increase in F_{ROH} was associated with a 68% [95% CI 55-78%] decrease in the odds of survival. However, the strength of inbreeding depression is dynamic across the lifespan. We estimate depression to peak in young adults, to decrease into older ages and to be weaker in lambs, where inbreeding effects are possibly buffered by maternal care. Finally, using a genome-wide association scan on ROH, we show that inbreeding causes depression predominantly through many loci with small effects, but we also find three regions in the genome with putatively strongly deleterious mutations. Our study reveals population and genome-wide patterns of homozygosity caused by inbreeding and sheds light on the strength, dynamics and genetic architecture of inbreeding depression in a wild mammal population.

Introduction

Inbreeding depression, the reduced fitness of offspring from related parents, has been a core theme in evolutionary and conservation biology since Darwin [1]. The detrimental effects of inbreeding on a broad range of traits, individual fitness and population viability have now been recognized all across the animal and plant kingdoms [1–9]. However, despite the ubiquity of inbreeding depression, we still know very little about its most fundamental features in wild populations [7,10]: What are the genomic patterns of homozygosity caused by inbreeding? How strong is inbreeding depression in fitness and how do its effects change across different life stages? What is the distribution of effect sizes at loci causing inbreeding depression?

Inbreeding decreases fitness because it increases the fraction of the genome which is homozygous and identical-by-descent (IBD). This unmasks the effects of (partially-) recessive deleterious alleles or in rarer cases may decrease fitness at loci with heterozygote advantage [4,11]. While the probability of IBD at a genetic locus was traditionally estimated as the expected inbreeding coefficient based on a pedigree [12,13], modern genomic approaches enable us to gain a much more detailed picture. Genome-wide markers or whole genome sequences are now unraveling the genomic mosaic of homo- and heterozygosity and, unlike pedigree-based approaches, capture individual variation in homozygosity due to the stochastic effects of Mendelian segregation and recombination [10,14]. This makes it possible to quantify realized rather than expected individual inbreeding, and can provide insights into how inbreeding causes IBD along the genome [15,16].

An intuitive and powerful way of measuring IBD is through runs of homozygosity (ROH), which are long stretches of homozygous genotypes [17]. ROH arise when two IBD haplotypes come together, which happens more frequently with increasing parental relatedness. However, ROH do not only originate from recent inbreeding, but can also emerge when shorter IBD haplotypes are inherited from apparently unrelated individuals due to background relatedness in the population. Consequently, ROH are ubiquitous even in outbred human populations [18], and in cases of strong inbreeding can stretch along whole chromosomes, as observed in some Scandinavian wolves [15]. The proportion of the autosomal genome in ROH (F_{ROH}) is an estimate of realized individual inbreeding F [19] and has been used to uncover inbreeding depression in a wide range of traits in humans and farm animals [5,20,21]. While F_{ROH} condenses the information about an individual's IBD into a single number, the genomic location of ROH reflects where the genome is homozygous due to inbreeding and can therefore help to elucidate the genetic basis of inbreeding depression [10,22].

A major challenge towards a better understanding of inbreeding depression is in mapping the underlying loci and estimating their effect sizes [10]. While simple recessive disease loci are relatively straightforward to identify through homozygosity mapping [23,24], quantifying the genetic basis of inbreeding depression in fitness and complex traits requires large samples in addition to dense genomic data [22]. As a consequence, the genetic architecture of inbreeding depression has mostly been studied in humans and livestock [25,26]. However, individual fitness will be different under natural conditions and consequently there is a need to study inbreeding depression in wild populations to understand its genetic basis in an evolutionary and ecological context. To date, only a handful of studies have estimated inbreeding depression using genomic data in the wild [27–31]. While these studies show that inbreeding depression in wild populations is more prevalent and more severe than previously thought, all of them used genome-wide inbreeding coefficients and did not explore the underlying genetic basis of depression.

Here, we combined long-term life-history data for 5952 free-living Soay sheep from the St. Kilda archipelago, Scotland, with over 417K partially imputed genome-wide SNP markers for a detailed genomic analysis of inbreeding depression. First, we quantified the genomic consequences of inbreeding through patterns of ROH among individuals and across the genome. We then calculated individual genomic inbreeding coefficients F_{ROH} to model inbreeding depression in annual survival and estimate its strength and dynamics across the lifetime. Finally, we explored the genetic architecture of inbreeding depression using a mixed-model based genome-wide association scan on ROH to shed light on whether depression is caused by many loci with small effects, few loci with large effects or a mixture of both.

Results

Study population. Soay sheep are descendants of early Bronze Age sheep and have lived on the island of Soay in the St Kilda Archipelago for thousands of years [32]. Although the Soays have been largely unmanaged, there is written and genomic evidence of an admixture event with the now extinct Dunface breed approximately 150 years or 32 generations ago [33]. Since 1985, the sheep inhabiting the Village Bay area of Hirta have been part of a long-term individual-based study [32]. Annual survival is assessed through routine mortality checks which are conducted throughout the year, and over 80% of sheep in the study area are found after their death [27]. For all following analyses we focused on a subset of 5952 sheep for which complete annual survival data and genomic data

were available. While many Soay sheep die early, some individuals live up to 15 years, resulting in a total of 15889 observations for annual survival (Supplementary Figure 1).

Genotyping and imputation. All study individuals have been genotyped on on the Illumina Ovine SNP50 BeadChip containing 51,135 SNP markers. In addition, 189 individuals have been genotyped on the Ovine Infinium High-Density chip containing 606,066 SNPs. To increase the genomic resolution for our analyses, we combined autosomal genotypes from both SNP chips with pedigree information to impute missing SNPs in individuals genotyped at lower marker density using AlphaImpute [34]. Cross-validation showed that imputation was successful, with a median of 99.3% correctly imputed genotypes per individual (Supplementary Table 1). Moreover, the inferred inbreeding coefficients F_{ROH} were very similar when comparing individuals genotyped on the high-density chip (median F_{ROH} = 0.239) and individuals with imputed SNPs (median F_{ROH} = 0.241), indicating no obvious bias in the abundance of inferred ROH based on imputed data (Supplementary Figure 2). After quality control, the genomic dataset contained 417,373 polymorphic and autosomal SNPs with a mean minor allele frequency (MAF) of 23% and a mean call rate of 99.5% across individuals.

Patterns of inbreeding in the genome. We first explored how inbreeding and a long-term small population size (estimated N_e = 194, [35]) shaped patterns of ROH in Soay sheep (Figure 1). Individuals had a mean of 194 ROH (sd = 11.6) longer than 1.2 Mb, which on average made up 24% of the autosomal genome (i.e. mean F_{ROH} = 0.24, range = 0.18-0.50, Supplementary Figure 3). IBD in the 1% most inbred individuals compared to the 1% least inbred individuals was characterized through longer ROH (mean: 5.27 Mb vs. 2.76 Mb), and slightly more abundant ROH (mean: 183 vs. 174). Figure 1A contrasts ROH longer than 5 Mb between the seven most and least inbred individuals, illustrating large differences in ROH length and coverage. The frequency of ROH in the population also varied widely across the genome (Figure 1B). We scanned ROH in the population in non-overlapping 500Kb windows, revealing regions with high ROH prevalence (ROH islands) and low ROH prevalence (ROH deserts) on every chromosome (Figure 1B). The top ROH island on chromosome 1 (227-227.5Mb) contained ROH in 87% of individuals, while only 4.4% of individuals had an ROH in the top ROH desert on chromosome 11 (58.5-59Mb, see Supplementary Table 2 for a list of the top ROH deserts and islands). Patterns of ROH on most chromosomes were shaped by recombination rate variation (Supplementary Figure 4). On average across the genome, a standardized (z-transformed) unit increase in recombination rate (measured as the summed fraction

of recombinants *r* in a window) was associated with a 2.3% decrease in ROH (*ß* [95% confidence interval] = -0.023 [-0.026, -0.019], Supplementary Table 3 for model details).

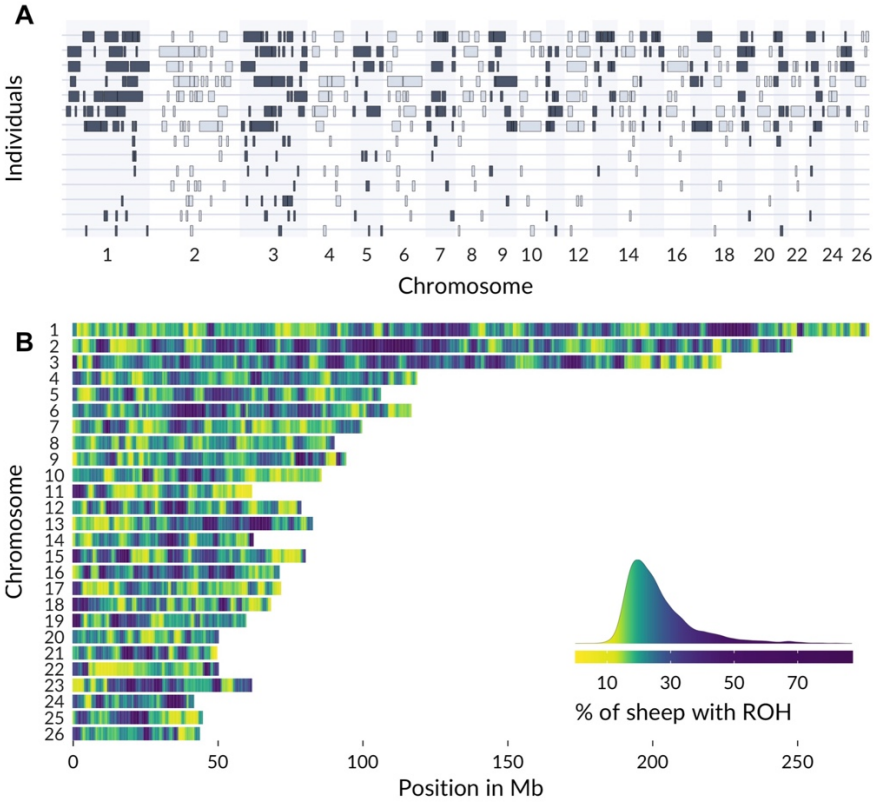

Figure 1: ROH variation (A) among the seven most and least inbred individuals and (B) across the Soay sheep genome. Panel A shows ROH longer than 5 Mb in the seven individuals with the highest F_{ROH} in the seven top rows and the seven individuals with the lowest F_{ROH} in the seven bottom rows. Panel B shows the genome-wide ROH prevalence among all 5952 individuals in non-overlapping 500Kb windows. The colour gradient on Panel B has been scaled according to the ROH prevalence distribution, which is shown as a density plot in the figure legend.

Inbreeding depression in survival. Survival is a key fitness component. In Soay sheep, more than half of all individuals die over their first winter, minimizing their chances to reproduce (Supplementary Figure 1). The distribution of individual inbreeding coefficients F_{ROH} in different age classes revealed that highly inbred individuals rarely survive their early years of life and never reach old ages (Figure 2A). We modeled this using a binomial animal model with annual survival as a response, including 15889 observations for 5952 sheep over more than three decades (see Methods for details). The effect of inbreeding on survival was strong: A 10% increase in F_{ROH} was associated with a 68% reduction in the odds of survival (*ß* [95% credible interval, CI] = 0.32 [0.22, 0.45]). Over the lifetime, inbreeding depression becomes weaker, with the slope of the interaction between F_{ROH} and age predicting an increase in the odds of survival (*ß* [CI] = 1.19 [1.06, 1.32]). In addition, the

slope of the interaction between F_{ROH} and being a lamb (β [CI] = 1.94 [1.05, 3.34]) indicates that inbreeding depression is weaker in lambs, though with considerable uncertainty (Figure 2B). As model estimates for odds of survival are not easy to interpret, we plotted the predicted effects of F_{ROH} on survival at different life stages (Figure 2C). Lambs (age 0) have a substantially lower survival probability but the curve is on average less steep than for individuals at age one, reflecting stronger depression in yearlings. Moreover, the three predicted survival curves for the age classes one, four and seven differ in slopes, reflecting the estimated decrease of inbreeding depression across life. A detailed list of the model estimates including the variable coding and standardization is shown in Supplementary Table 4. As an alternative way to visualize the lifetime dynamics of inbreeding depression, we also fitted separate models for each age class, which show essentially the same pattern (Supplementary Figure 5). Finally we estimated the genetic load in Soay sheep through the diploid number of lethal equivalents 2B. Lethal equivalents are a concept rooted in population genetics, where one lethal equivalent is equal to a group of mutations which, if dispersed across individuals, would on average cause one death [36]. We followed suggestions by Nietlisbach et al [37] and refitted the survival model with a Poisson distribution and logarithmic link function using a simplified model structure without interactions for a better comparability across studies. This gave an estimate of 2B = 4.57 (95% CI 2.61-6.55) lethal equivalents for Soay sheep annual survival.

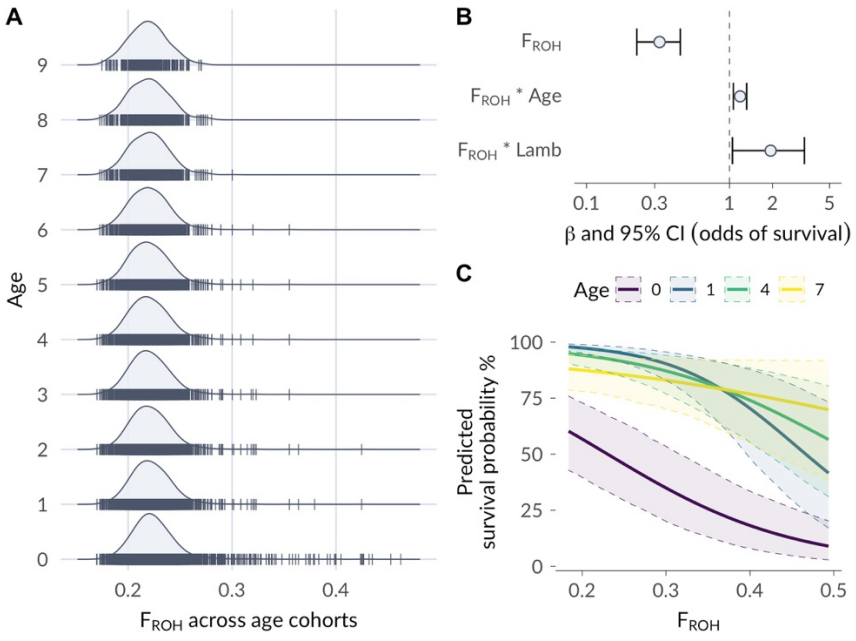

Figure 2: Inbreeding depression in annual survival. Panel A shows the distributions of inbreeding coefficients F_{ROH} in Soay sheep age classes ranging from 0 to 10 years. Panel B shows the model estimates (posterior mean and 95% CI) for individual inbreeding F_{ROH} and its interaction with age and being a lamb. F_{ROH} has been centered around its mean and transformed so that a unit change and hence the model estimate reflects the change in survival probability for a 0.1 increase in F_{ROH} from the mean. Panel C shows the predicted

survival probability and 95% CI over the range of inbreeding coefficients F_{ROH} for lambs (age 0), and 1, 4 and 7-year old individuals respectively, while holding sex and twin constant at 1 (male) and 0 (no twin). The predictions for age classes 1, 4, and 7 exceed the range of the data (panel A) but are shown across the full range for comparability.

Genetic architecture of inbreeding depression. To quantify the survival consequences of being IBD at each SNP location, we used a modified genome-wide association study (GWAS). Unlike in traditional GWAS where p-values of additive SNP effects are of interest, we analysed a binary fixed effect of ROH status, which indicates whether a focal SNP is in an ROH or not [25,26,38]. We fitted a binomial mixed model of annual survival for each SNP, with individual ROH status at the focal SNP position as fixed effect, and controlled for the additive SNP effect and mean individual inbreeding F_{ROH} (based on all autosomes except for the focal chromosome) alongside a range of other individual traits and environmental effects (see Methods for details). Under the null hypothesis that ROH status does not have an effect on survival at any SNP position, we would expect a 50/50 distribution of negative and positive GWAS effects, as all model estimates are due to chance. In contrast, we found many more negative than positive effects of ROH status on survival across the genome than expected by chance (Figure 3A, 3B; 247K neg. vs. 171K pos.; exact binomial test $p = 2.2 * 10^{-16}$). Using binomial GLMs with effect direction as binary response variable, we also estimated an increasing proportion of negative effects among larger estimates (β [95% CI] = 0.27 [0.26, 0.28]) and lower p-values (β [95% CI] = 0.95 [0.94, 0.96]). Consequently, it is likely that many loci with small effects contribute to inbreeding depression in survival. Moreover, ROH status reached genome-wide significance in three regions on chromosomes 3, 10, and 23, revealing putative large effect mutations (Figure 3C, Supplementary Table 5). While largely deleterious recessive variants might be expected to occur in regions of elevated heterozygosity where they are rarely expressed in their homozygous state, we did not observe clear common patterns of genetic diversity in these three regions, although heterozygosity is slightly elevated and ROH frequency is lower around the top SNPs on chromosomes 10 and 23 (Supplementary Figure 6).

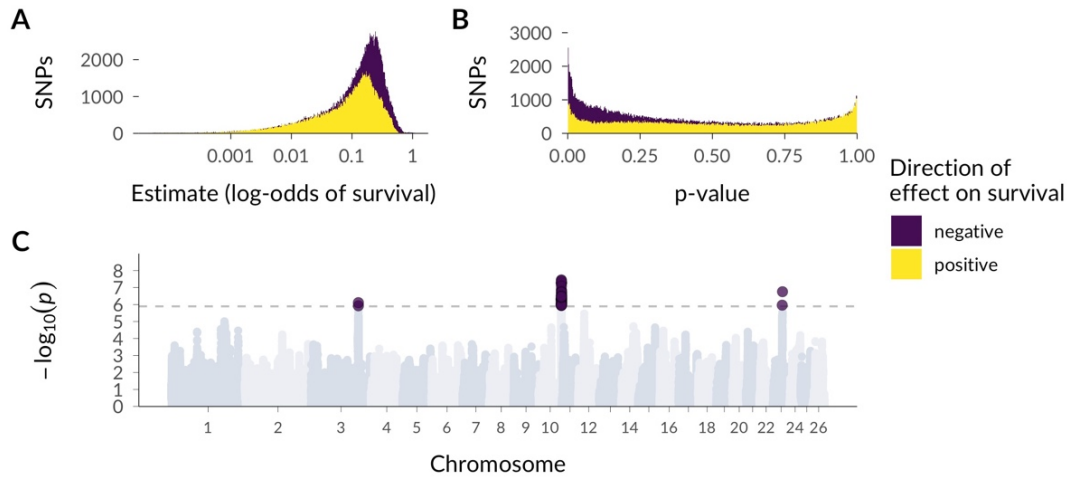

Figure 3: GWAS of SNP-wise ROH status effect on annual survival. Regional inbreeding depression was conceptualised and tested as a binary fixed effect of whether a SNP was part of an ROH (and hence IBD) or not. Panel A and B show the distribution of effect sizes and p-values for this SNP-wise ROH effect. The yellow histograms showing positive effects are superimposed on top of the purple histograms showing negative effects to highlight that there was a substantially larger proportion of negative ROH status effects than expected by chance. Panel C shows a Manhattan plot of the SNP-wise ROH status p-values across the genome. The dotted line marks the genome-wide significance threshold for a Bonferroni correction which was based on the effective number of tests when accounting for LD. All genome-wide significant p-values were associated with negative effects on survival.

Discussion

The Soay sheep on St. Kilda have existed at a small population size and relative isolation for thousands of years [32]. As a consequence, levels of IBD are high in the population and ROH make up nearly a quarter of the average autosomal Soay sheep genome. This is more than three times as high as the average F_{ROH} estimated across 78 mammal species based on genome-sequence data [39], but still slightly lower than in some extremely inbred and very small populations such as mountain gorillas [40], Scandinavian grey wolves [15] or Isle Royale wolves [41]. The prevalence of ROH varied substantially across the genome and was broadly shaped by recombination rate variation, which is known to impact ROH patterns alongside other factors such as gene density and selection [18,42,43]. We showed that most chromosomes contain both deserts where ROH are rare and islands where ROH are common. In the most extreme regions as few as 4% and up to 87% of individuals had ROH and this has potential implications for the distribution of deleterious mutations. ROH islands are likely to contain few recessive deleterious alleles, as these are regularly exposed to selection when homozygous and hence likely to be purged from the population. Expectations for deleterious mutations in ROH deserts are more difficult to formulate because the (near-) absence of ROH could

246 be caused by several mechanisms, such as a high recombination rate or balancing selection.
247 However, a lack of ROH could potentially pinpoint regions harbouring lethal or semi-lethal alleles,
248 though this has only been demonstrated in farm animals using very large sample sizes (e.g. Jenko
249 et al., 2019).
250
251 We have only recently begun to understand the precise consequences of inbreeding for individual
252 fitness in natural populations. In Soay sheep, we found that the odds of survival decrease by 68%
253 with a mere 10% increase in F_{ROH}, adding to a small yet growing body of genomic studies showing
254 that inbreeding depression is stronger in wild populations than previously thought [27–29,31]. Other
255 recent examples include lifetime breeding success in red deer, which is reduced by up to 95% in
256 male offspring from half-sib matings [31] and lifetime reproductive success in helmeted honeyeaters,
257 which is up to 90% lower with a 9% increase in homozygosity [29]. The traditional way to compare
258 inbreeding depression among studies is to estimate the genetic load of a population using lethal
259 equivalents [36], although differences in methodology and inbreeding estimates often do not allow
260 direct comparisons [37]. We estimated the diploid number of lethal equivalents 2B for Soay sheep
261 annual survival at 4.57 (95% CI 2.61-6.55). This is a low to moderate inbreeding load compared to
262 other estimates from wild mammals obtained from appropriate statistical models [37], but
263 corroborates with theoretical expectations of lower genetic load in small populations [7] and a recent
264 comparative study estimating lower genetic load in smaller mammal populations [45].
265
266 Inbreeding depression is dynamic across life, and genomic measures are starting to unravel how
267 inbreeding depression affects fitness at different life-stages in wild populations [27,28,31]. Under the
268 mutation accumulation hypothesis [46], the adverse effects of deleterious mutations expressed late in
269 life should become stronger as selection becomes less efficient. This can theoretically increase the
270 effects of inbreeding depression later in life [47], although empirical evidence is sparse [48,49]. In contrast
271 to the idea of mutation accumulation, we showed that inbreeding depression in Soay sheep
272 generally becomes weaker over the lifetime. In addition, the sample for each successive age class
273 consists of increasingly outbred individuals (Figure 2C) due to a higher death rate among inbred
274 individuals earlier in life. This suggests that the effects of intragenerational purging [50] might
275 outweigh mutation accumulation in shaping the dynamics of inbreeding depression across the
276 lifetime. As a notable exception, we estimated inbreeding depression to be slightly weaker in lambs,
277 which may be because it is partially buffered by maternal care. Parental care has indeed been shown
278 to reduce inbreeding depression in burying beetles [51], but there is only limited evidence in mammals

to date [52,53]. Overall, we estimated inbreeding depression over a Soay sheep's life to start slightly weaker in lambs, reaching its maximum in early adulthood and then decrease thereafter.

The effect size distribution of loci underpinning inbreeding depression has to our knowledge not been studied in wild populations using fitness data, although deleterious mutations have been predicted from sequencing data, for example in ibex and Isle Royale wolves [41,54]. Theoretical predictions about the relative importance of weakly and strongly deleterious (partially-) recessive alleles will depend on many factors, such as the distribution of dominance and selection coefficients for mutations relative to the effective population size, and the frequency of inbreeding [55,56]. However, we could expect that small populations purge largely deleterious recessive mutations more efficiently as these are more frequently exposed to selection in the homozygous state [7,57,58], while weakly deleterious mutations can more often drift to higher frequencies. We estimated the effect of ROH status on Soay sheep survival at every SNP position within a GWAS framework. The effect size distribution contained predominantly negative effects of ROH status on survival, particularly towards larger effect sizes, showing that likely many alleles with weakly deleterious effects (or low frequencies) contribute to inbreeding depression in survival.

Three regions in the genome also harboured putatively strongly deleterious alleles. This is unexpected, as Soay sheep have a long-term small population size with an estimated N_e of 197 [35], and highly deleterious recessive mutations should be rapidly purged. On the one hand however, it is possible that genetic drift counteracted the effects of purifying selection and allowed deleterious mutations to increase in frequency and be detected in a GWAS. On the other hand, a relatively recent admixture event with the Dunface sheep breed around 150 years ago [33] could have introduced deleterious variants into the population and recent selection has not been efficient enough to purge them from the population yet. Identifying the loci carrying these strongly deleterious recessive alleles will be challenging as ROH overlapping a given SNP vary in length among individuals, which makes it difficult to pinpoint an exact effect location. Nevertheless, it is possible to identify the haplotypes harbouring deleterious recessive alleles with large effects and monitor their frequency changes in real time in natural populations, or select out individuals carrying them in conservation breeding programs. To sum up, our study showed how genome-wide marker information for a large sample of individuals with known fitness can deepen our understanding of the genetic architecture and lifetime dynamics of inbreeding depression in the wild.

Methods

Study population, pedigree assembly and annual survival measurements. The Soay sheep is a primitive sheep breed descended from Bronze Age domestic sheep and has lived unmanaged on the St. Kilda archipelago, Scotland for thousands of years. When the last human inhabitants left St. Kilda in 1932, 107 Soays were transferred to the largest island, Hirta, and have roamed the island freely and unmanaged ever since. The population increased and fluctuates nowadays between 600 and 2200 individuals. A part of the population in the Village Bay area of Hirta (57 49'N, 8 34'W) has been the subject of a long-term individual based study since 1985 [32]. Most individuals born in the study area (95%) are ear-tagged and DNA samples are obtained from ear punches or blood sampling. Routine mortality checks are conducted throughout the year with peak mortality occurring at the end of winter and beginning of spring. Overall, around 80% of deceased animals are found [27]. For the analyses in this paper, survival was defined as dying (0) or surviving (1) from the 1st May of the previous year to the 30th April of that year, with measures available for 5952 individuals from 1979 to 2018. We focused on annual measures as this allowed us to incorporate the effects of age and environmental variation.

To assemble the pedigree, we inferred parentage for each individual using 438 unlinked SNP markers from the Ovine SNP50 BeadChip, on which most individuals since 1990 have been genotyped [59]. Based on these 438 markers, we inferred pedigree relationships using the R package Sequoia [60]. In the few cases where no SNP genotypes were available, we used either field observations (for mothers) or microsatellites [61]. All animal work was carried out according to UK Home Office procedures and was licensed under the UK Animals (Scientific Procedures) Act of 1986 (Project License no. PPL70/8818).

Genotyping. We genotyped a total of 7,700 Soay on the Illumina Ovine SNP50 BeadChip containing 51,135 SNP markers. To control for marker quality, we first filtered for SNPs with minor allele frequency (MAF) > 0.001, SNP locus genotyping success > 0.99 and individual sheep genotyping success > 0.95. We then used the check.marker function in GenABEL version 1.8-0 [62] with the same thresholds, including identity by state with another individual < 0.9. This resulted in a dataset containing 39,368 polymorphic SNPs in 7700 sheep. In addition, we genotyped 188 sheep on the Ovine Infinium HD SNP BeadChip containing 606,066 SNP loci. These sheep were specifically selected to maximise the genetic diversity represented in the full population as described in Johnston et al. [63], and underwent the same quality control as above, resulting in 430,702 polymorphic SNPs for 188 individuals. All genotype positions were based on the Oar_v3.1 sheep genome assembly (GenBank assembly ID GCA_000298735.1 [64])

Genotype imputation. In order to impute genotypes to high density, we merged the datasets from the 50K SNP chip and from the HD SNP chip using PLINK v1.90b6.12 with –bmerge [65]. This resulted in a dataset with 436,117 SNPs including 33,068 SNPs genotyped on both SNP chips. For genotype imputation, we discarded SNPs on the X chromosome and focused on the 419,281 SNPs located on autosomes. The merged dataset contained nearly complete genotype information for 188 individuals which have been genotyped on the HD chip, and genotypes at 38,130 SNPs for 7700 individuals which have been genotyped on the 50K chip. To impute the missing SNPs, we used AlphaImpute v1.98 [34], which combines information on shared haplotypes and pedigree relationships for phasing and genotype imputation. AlphaImpute works on a per-chromosome basis, and phasing and imputation are controlled using a parameter file (for the exact parameter file, see analysis code). Briefly, we phased individuals using core lengths ranging from 1% to 5% of the SNPs on a given chromosome over 10 iterations, resulting in a haplotype library. Based on the haplotype library, missing alleles were imputed using the heuristic method over five iterations which allowed us to use genotype information imputed in previous iterations. We only retained imputed genotypes for which all phased haplotypes matched and did not allow for errors. We also discarded SNPs with call rates below 95% after imputation. Overall, this resulted in a dataset with 7691 individuals, 417,373 SNPs and a mean genotyping rate per individual of 99.5 % (range 94.8%-100%).

To evaluate the accuracy of the imputation we used 10-fold leave-one-out cross-validation. In each iteration, we masked the genotypes unique to the high-density chip for one random individual that had been genotyped at high-density (HD) and imputed the masked genotypes. This allowed a direct comparison between the true and imputed genotypes. The imputation accuracy of the HD individuals should reflect of the average imputation accuracy across the whole population, because HD individuals were selected to be representative of the genetic variation observed across the pedigree (see Johnston et al., 2016 for details).

ROH calling and individual inbreeding coefficients. The final dataset contained genotypes at 417,373 SNPs autosomal SNPs for 5925 individuals for which annual survival data was available. We called runs of homozygosity (ROH) with a minimum length of 1200Kb and spanning at least 50 SNPs with the --homozyg function in Plink [65] and the following parameters: --homozyg-window-snp 50 --homozyg-snp 50 --homozyg-kb 1200 --homozyg-gap 300 --homozyg-density 200 --homozyg-window-missing 2 --homozyg-het 2 --homozyg-window-het 2. We chose 1200Kb as the minimum ROH length because between-individual variability in ROH abundance becomes very low for shorter ROH. Moreover, ROH of length 1200Kb extend well above the LD half decay in the population, thus

capturing variation in IBD due to more recent inbreeding rather than linkage disequilibrium (Supplementary Figure 7). The minimum ROH length of 1200Kb also reflects the expected length when the underlying IBD haplotypes had a most recent common ancestor haplotype 32 generations ago, calculated as (100 / (2*g)) cM / 1.28 cM/Mb where g is 32 generations and 1.28 is the sex-averaged genome-wide recombination rate in Soay sheep [63,66]. We then calculated individual inbreeding coefficients F_{ROH} by summing up the total length of ROH for each individual and dividing this by the total autosomal genome length (2,452Mb).

ROH landscape and recombination rate variation. To quantify variation in population-wide ROH prevalence across the genome, we used a sliding window approach. We first calculated the number of ROH overlapping each SNP position in the population using PLINK --homozyg. We then calculated the mean number of ROH overlapping SNPs in 500 Kb non-overlapping sliding windows in the population (Figure 1B). To estimate the top 0.5% ROH deserts and islands, we discarded windows with less than 35 SNPs (the percentile of windows with the lowest SNP density). To estimate the relationship between ROH prevalence and recombination rate we then quantified the recombination rate in 500Kb window. We calculated recombination rate as the sum of the recombination fractions *r* between consecutive loci in each window, using data from the Soay sheep linkage map [63]. We then constructed a linear mixed model in lme4 [67] with population-wide ROH prevalence per window as response, window recombination rate and chromosome size as fixed effects and chromosome ID as random intercept (Supplementary Table 3). The fixed effects in the model were standardised using z-transformation. To estimate confidence intervals, we used parametric bootstrapping implemented in the tidy function of the broom.mixed package [68].

Modelling inbreeding depression in survival. We modelled the effects of inbreeding depression in annual survival using a Bayesian animal model in INLA [69]. Annual survival data consists of a series of 1s followed by a 0 in the year of a sheep's death, or only a 0 if it died as a lamb, and we consequently used a binomial distribution with a logit link for the model. We used the following model structure:

$$\Pr(surv_i = 1) = logit^{-1}(\beta_0 + F_{ROH_i}\beta_1 + age_i\beta_2 + sex_i\beta_3 + twin_i\beta_4 + lamb_i\beta_5 + F_{ROH_i}age_i\beta_6 + F_{ROH_i}lamb_i\beta_7 + \alpha_j^{capture\ year} + \alpha_k^{birth\ year} + \alpha_l^{id} + u_l^{ped})$$

$$\alpha_j^{capture\ year} \sim N(0, \sigma^2_{year}), \qquad for\ j = 1, \dots, 40$$

$$\alpha_k^{birth\ year} \sim N(0, \sigma^2_{birth\ year}), \qquad for\ k = 1, \dots, 40$$

$$\alpha_l^{id} \sim N(0, \sigma_{id}^2), \quad for\ l = 1, \dots, 5925$$

$$u_l^{ped} \sim N(0, A\sigma_A^2) \quad for\ l = 1, \dots, 5925$$

Here, $\Pr(surv_i = 1)$ is the probability of survival for observation *i*, which depends on the intercept β_0, a series of fixed effects β_1 to β_7 , the random effects α which are assumed to be normally distributed with mean 0 and variance σ^2 and the breeding values u_l^{ped} which have a dependency structure corresponding to the pedigree, with a mean of 0 and a variance of $A\sigma_A^2$, where A is the relationship matrix and σ_A^2 is the additive genetic variance. As fixed effects, we fitted the individual inbreeding coefficient F_{ROH} (continuous), the *age* of the individual (continuous), *sex* (0 = female, 1 = male), a variable indicating whether an individual was born as a *twin* (0 = singleton, 1 = twin) and whether the individual is a *lamb* before its first year of age (0 = not a lamb, 1 = lamb). We also fitted an interaction term of F_{ROH} with *age* to estimate how inbreeding depression changes across the lifetime and an interaction term of F_{ROH} with *lamb* to estimate potential differences in inbreeding depression in lambs, as they receive maternal care which could ameliorate inbreeding depression. As random intercepts we fitted the birth year of an individual, the capture year to account for survival variation among years and the sheep identity to account for repeated measures. Finally, we controlled for additive genetic relatedness by including a covariance structure proportional to the pedigree relatedness matrix, as has previously been described for INLA models [70]. For all random effects, we used log-gamma priors with both shape and inverse-scale parameter values of 0.5.

To be able to interpret the slopes of the main effects of F_{ROH} and age despite their interactions at the mean value of the respective other variable (rather than at 0), we centered both variables [71,72]. Furthermore, we transformed F_{ROH} from its original range 0-1 to 0-10, which allowed us to directly interpret model estimates as resulting from a 10% increase in genome-wide IBD rather than the difference between a completely outbred and a completely inbred individual. Finally, we report model estimates on the response scale (as odds of survival) in the main paper, and on the link scale (as log-odds of survival) in the Supplementary Material.

Estimating lethal equivalents. The traditional way of comparing inbreeding depression among studies is to quantify the inbreeding load in terms of lethal equivalents, i.e. a group of genes which would cause on average one death if dispersed in different individuals and made homozygous [36]. However, differences in statistical methodology and inbreeding measures make it difficult to compare the strength of inbreeding depression in terms of lethal equivalents among studies [37]. Here, we used the approach suggested by Nietlisbach et al. (2019) and refitted the survival animal model with a Poisson distribution and a logarithmic link function. We were interested in lethal

equivalents for the overall strength of inbreeding depression rather than its lifetime dynamics, so we fitted a slightly simplified animal model with F_{ROH}, age, age^2, twin and sex as fixed effects and birth year, capture year, individual id and pedigree relatedness as random effects. The slope of F_{ROH} estimates the decrease in survival due to a 10% increase in F_{ROH}, so we calculated the number of diploid lethal equivalents 2B as $-(\beta_{FROH})/0.10 * 2$ where β_{FROH} is the Poisson model slope for F_{ROH}.

Mapping inbreeding depression. To map the effects of inbreeding depression in survival across the genome, we used a modification of a genome-wide association study [25,26,38]. For each of the ~417K SNPs, we fitted a binomial mixed model with logit link in lme4 [67] with the following model structure:

$$\Pr(surv_i = 1) = logit^{-1}(\beta_0 + SNP_{ROH_i}\beta_1 + SNP_{ADD_i}\beta_2 + F_{ROH_{mod_i}}\beta_3 + age_i\beta_4 + age_i^2\beta_5 + sex_i\beta_6 + twin_i\beta_7 + \beta_{8-15}PC_{1-7} + \alpha_j^{capture\ year} + \alpha_k^{birth\ year} + \alpha_l^{id})$$

$$\alpha_j^{capture\ year} \sim N(0, \sigma^2_{capture\ year}), \quad for\ j = 1, \dots, 40$$
$$\alpha_k^{birth\ year} \sim N(0, \sigma^2_{birth\ year}), \quad for\ k = 1, \dots, 40$$
$$\alpha_l^{id} \sim N(0, \sigma^2_{id}), \quad for\ l = 1, \dots, 5925$$

Where the effect of interest is that of SNP_{ROH}, a binary variable indicating whether a SNP is in an ROH (SNP_{ROH} = 1) or not (SNP_{ROH} = 0). SNP_{ADD} is the additive effect for the focal SNP (0,1,2 for homozygous, heterozygous, homozygous for the alternative allele, respectively), and controls for the possibility that a potential negative effect of ROH status is simply an additive effect. $F_{ROH_{mod}}$ is the mean inbreeding coefficient of the individual based on all chromosomes except for the chromosome where the focal SNP is located. We fitted F_{ROH} as we were interested in the effect of ROH status at a certain locus (SNP_{ROH}), on top of the average individual inbreeding coefficient. Sex and twin are again binary variables representing the sex of the individual and whether it is a twin. Age and age^2 control for the linear and quadratic effects of age, and are fitted as continuous covariates. Because it was computationally impractical to fit 417K binomial animal models with our sample size and because the additive genetic variance in survival is negligible (see Supplementary Table 4), we did not fit an additive genetic effect. Instead, we used the top 7 principal components of the variance-standardized additive relationship matrix ($PC_{1\text{-}7}$) as fixed effects [65]. Again, we added birth year, capture year and individual id as random effects. For each fitted model, we extracted the estimated slope of SNP_{ROH} and its p-value calculated based on a Wald-Z test. To determine a threshold for genome-wide significance we used the 'simpleM' procedure [73]. The method uses composite linkage

483 disequilibrium to create a SNP correlation matrix and calculates the effective number of independent
484 tests. We then used this value for a Bonferroni correction [74] of p-values resulting in a genome-wide
485 significance threshold of $p < 1.28 * 10^{-6}$.
486
487 **Data availability**
488 Data will be deposited on Dryad upon acceptance.
489
490 **Code availability**
491 All code was written in R 3.6.1 [75] and all plots were made with ggplot2 [76]. The full analysis code is
492 available on GitHub (https://github.com/mastoffel/sheep_ID).
493
494 **Acknowledgements**
495 We thank the National Trust for Scotland for permission to work on St. Kilda and QinetiQ, Eurest and
496 Kilda Cruises for logistics and support. We thank I. Stevenson and many volunteers who have helped
497 with fieldwork on the island and all those who have contributed to keeping the project going. SNP
498 genotyping was conducted the Wellcome Trust Clinical Research Facility Genetic Core. This work
499 has made extensive use of the Edinburgh Compute and Data Facility (http://www.ecdf.ed.ac.uk/).
500 We thank John Hickey, Steve Thorn, Andrew Whalen and Martin Johnsson for help with the
501 imputation. We are grateful for discussions with David Clark, Jon Slate, Jisca Huisman, Jarrod
502 Hadfield, Peter Visscher, Anna Hewett, Deborah and Brian Charlesworth and the Wild Evolution
503 Group. We also thank Emily Humble for comments on an earlier draft of the manuscript. The project
504 was funded through an outgoing Postdoc fellowship from the German Science Foundation (DFG)
505 awarded to MAS and a Leverhulme Grant (RPG-2019-072) awarded to JMP and SEJ. Field data
506 collection has been supported by NERC over many years, and most of the SNP genotyping was
507 supported by an ERC Advanced Grant to JMP.
508
509
510
511

References

1. Darwin, C. *The effect of cross and self fertilization in the vegetable kingdom*. (John Murray, 1876).
2. Angeloni, F., Ouborg, N. J. & Leimu, R. Meta-analysis on the association of population size and life history with inbreeding depression in plants. *Biological Conservation* **144**, 35–43 (2011).
3. Bozzuto, C., Biebach, I., Muff, S., Ives, A. R. & Keller, L. F. Inbreeding reduces long-term growth of Alpine ibex populations. *Nature ecology & evolution* **3**, 1359–1364 (2019).
4. Charlesworth, D. & Willis, J. H. The genetics of inbreeding depression. *Nature Reviews Genetics* (2009).
5. Clark, D. W. *et al.* Associations of autozygosity with a broad range of human phenotypes. *Nature Communications* **10**, 1–17 (2019).
6. Crnokrak, P. & Roff, D. A. Inbreeding depression in the wild. *Heredity* **83**, 260–270 (1999).
7. Hedrick, P. W. & Garcia-Dorado, A. Understanding inbreeding depression, purging, and genetic rescue. *Trends in ecology & evolution* **31**, 940–952 (2016).
8. Keller, L. Inbreeding effects in wild populations. *Trends in ecology & evolution* **17**, 230–241 (2002).
9. Ralls, K., Ballou, J. D. & Templeton, A. Estimates of lethal equivalents and the cost of inbreeding in mammals. *Conservation biology* **2**, 185–193 (1988).
10. Kardos, M., Taylor, H. R., Ellegren, H., Luikart, G. & Allendorf, F. W. Genomics advances the study of inbreeding depression in the wild. *Evolutionary applications* **9**, 1205–1218 (2016).
11. Hedrick, P. W. What is the evidence for heterozygote advantage selection? *Trends in ecology & evolution* **27**, 698–704 (2012).
12. Pemberton, J. Measuring inbreeding depression in the wild: the old ways are the best. *Trends in ecology & evolution* **19**, 613–615 (2004).
13. Wright, S. Coefficients of Inbreeding and Relationship. *The American Naturalist* **56**, 330–338 (1922).
14. Franklin, I. R. The distribution of the proportion of the genome which is homozygous by descent in inbred individuals. *Theoretical population biology* **11**, 60–80 (1977).
15. Kardos, M. *et al.* Genomic consequences of intensive inbreeding in an isolated wolf population. *Nature Ecology & Evolution* **2**, 124–131 (2018).
16. Kardos, M., Luikart, G. & Allendorf, F. W. Measuring individual inbreeding in the age of genomics: marker-based measures are better than pedigrees. *Heredity* **115**, 63 (2015).

17. Broman, K. W. & Weber, J. L. Long homozygous chromosomal segments in reference families from the centre d'Etude du polymorphisme humain. *The American Journal of Human Genetics* **65**, 1493–1500 (1999).
18. Gibson, J., Morton, N. E. & Collins, A. Extended tracts of homozygosity in outbred human populations. *Hum Mol Genet* **15**, 789–795 (2006).
19. McQuillan, R. *et al.* Runs of homozygosity in European populations. *The American Journal of Human Genetics* **83**, 359–372 (2008).
20. Curik, I., Ferenčaković, M. & Sölkner, J. Inbreeding and runs of homozygosity: A possible solution to an old problem. *Livestock Science* **166**, 26–34 (2014).
21. Leroy, G. Inbreeding depression in livestock species: review and meta-analysis. *Animal Genetics* **45**, 618–628 (2014).
22. Ceballos, F. C., Joshi, P. K., Clark, D. W., Ramsay, M. & Wilson, J. F. Runs of homozygosity: windows into population history and trait architecture. *Nature Reviews Genetics* (2018).
23. Kijas, J. W. Detecting regions of homozygosity to map the cause of recessively inherited disease. in *Genome-wide association studies and genomic prediction* 331–345 (Springer, 2013).
24. Lander, E. S. & Botstein, D. Homozygosity mapping: a way to map human recessive traits with the DNA of inbred children. *Science* **236**, 1567–1570 (1987).
25. Ferenčaković, M., Sölkner, J., Kapš, M. & Curik, I. Genome-wide mapping and estimation of inbreeding depression of semen quality traits in a cattle population. *Journal of Dairy Science* **100**, 4721–4730 (2017).
26. Pryce, J. E., Haile-Mariam, M., Goddard, M. E. & Hayes, B. J. Identification of genomic regions associated with inbreeding depression in Holstein and Jersey dairy cattle. *Genetics Selection Evolution* **46**, (2014).
27. Bérénos, C., Ellis, P. A., Pilkington, J. G. & Pemberton, J. M. Genomic analysis reveals depression due to both individual and maternal inbreeding in a free-living mammal population. *Molecular ecology* **25**, 3152–3168 (2016).
28. Chen, N., Cosgrove, E. J., Bowman, R., Fitzpatrick, J. W. & Clark, A. G. Genomic consequences of population decline in the endangered Florida scrub-jay. *Current Biology* **26**, 2974–2979 (2016).
29. Harrisson, K. A. *et al.* Lifetime Fitness Costs of Inbreeding and Being Inbred in a Critically Endangered Bird. *Current Biology* **29**, 2711-2717.e4 (2019).

30. Hoffman, J. I. *et al.* High-throughput sequencing reveals inbreeding depression in a natural population. *Proceedings of the National Academy of Sciences of the United States of America* **111**, 3775–3780 (2014).
31. Huisman, J., Kruuk, L. E., Ellis, P. A., Clutton-Brock, T. & Pemberton, J. M. Inbreeding depression across the lifespan in a wild mammal population. *Proceedings of the National Academy of Sciences* **113**, 3585–3590 (2016).
32. Clutton-Brock, T. H. & Pemberton, J. M. *Soay sheep: dynamics and selection in an island population*. (Cambridge University Press, 2004).
33. Feulner, P. G. D. *et al.* Introgression and the fate of domesticated genes in a wild mammal population. *Molecular Ecology* **22**, 4210–4221 (2013).
34. Hickey, J. M., Kinghorn, B. P., Tier, B., van der Werf, J. H. & Cleveland, M. A. A phasing and imputation method for pedigreed populations that results in a single-stage genomic evaluation. *Genetics Selection Evolution* **44**, 9 (2012).
35. Kijas, J. W. *et al.* Genome-Wide Analysis of the World's Sheep Breeds Reveals High Levels of Historic Mixture and Strong Recent Selection. *PLOS Biology* **10**, e1001258 (2012).
36. Morton, N. E., Crow, J. F. & Muller, H. J. An estimate of the mutational damage in man from data on consanguineous marriages. *Proceedings of the National Academy of Sciences of the United States of America* **42**, 855 (1956).
37. Nietlisbach, P., Muff, S., Reid, J. M., Whitlock, M. C. & Keller, L. F. Nonequivalent lethal equivalents: Models and inbreeding metrics for unbiased estimation of inbreeding load. *Evolutionary applications* **12**, 266–279 (2019).
38. Keller, M. C. *et al.* Runs of homozygosity implicate autozygosity as a schizophrenia risk factor. *PLoS genetics* **8**, (2012).
39. Brüniche-Olsen, A., Kellner, K. F., Anderson, C. J. & DeWoody, J. A. Runs of homozygosity have utility in mammalian conservation and evolutionary studies. *Conservation Genetics* **19**, 1295–1307 (2018).
40. Xue, Y. *et al.* Mountain gorilla genomes reveal the impact of long-term population decline and inbreeding. *Science* **348**, 242–245 (2015).
41. Robinson, J. A. *et al.* Genomic signatures of extensive inbreeding in Isle Royale wolves, a population on the threshold of extinction. *Science Advances* **5**, eaau0757 (2019).
42. Wang, H., Lin, C.-H., Chen, Y., Freimer, N. & Sabatti, C. Linkage disequilibrium and haplotype homozygosity in population samples genotyped at a high marker density. *Human heredity* **62**, 175–189 (2006).

609 43. Pemberton, T. J. *et al.* Genomic patterns of homozygosity in worldwide human populations.
610 *The American Journal of Human Genetics* **91**, 275–292 (2012).
611 44. Jenko, J. *et al.* Analysis of a large dataset reveals haplotypes carrying putatively recessive lethal
612 and semi-lethal alleles with pleiotropic effects on economically important traits in beef cattle.
613 *Genetics Selection Evolution* **51**, 9 (2019).
614 45. van der Valk, T., de Manuel, M., Marques-Bonet, T. & Guschanski, K. Estimates of genetic load
615 in small populations suggest extensive purging of deleterious alleles. *bioRxiv* 696831 (2019).
616 46. Medawar, P. B. *An Unsolved Problem of Biology*. (H.K. Lewis, 1952).
617 47. Charlesworth, B. & Hughes, K. A. Age-specific inbreeding depression and components of
618 genetic variance in relation to the evolution of senescence. *Proceedings of the National*
619 *Academy of Sciences* **93**, 6140–6145 (1996).
620 48. Husband, B. C. & Schemske, D. W. Evolution of the magnitude and timing of inbreeding
621 depression in plants. *Evolution* **50**, 54–70 (1996).
622 49. Wilson, A. J. *et al.* Evidence for a genetic basis of aging in two wild vertebrate populations.
623 *Current Biology* **17**, 2136–2142 (2007).
624 50. Enders, L. S. & Nunney, L. Reduction in the cumulative effect of stress-induced inbreeding
625 depression due to intragenerational purging in Drosophila melanogaster. *Heredity* **116**, 304
626 (2016).
627 51. Pilakouta, N., Jamieson, S., Moorad, J. A. & Smiseth, P. T. Parental care buffers against
628 inbreeding depression in burying beetles. *Proceedings of the National Academy of Sciences*
629 **112**, 8031–8035 (2015).
630 52. Nielsen, J. F. *et al.* Inbreeding and inbreeding depression of early life traits in a cooperative
631 mammal. *Molecular Ecology* **21**, 2788–2804 (2012).
632 53. Wells, D. A., Cant, M. A., Nichols, H. J. & Hoffman, J. I. A high-quality pedigree and genetic
633 markers both reveal inbreeding depression for quality but not survival in a cooperative
634 mammal. *Molecular ecology* **27**, 2271–2288 (2018).
635 54. Grossen, C., Guillaume, F., Keller, L. F. & Croll, D. Purging of highly deleterious mutations
636 through severe bottlenecks in Alpine ibex. *Nature Communications* **11**, 1–12 (2020).
637 55. Bataillon, T. & Kirkpatrick, M. Inbreeding depression due to mildly deleterious mutations in
638 finite populations: size does matter. *Genetics Research* **75**, 75–81 (2000).
639 56. Glémin, S. How are deleterious mutations purged? Drift versus nonrandom mating. *Evolution*
640 **57**, 2678–2687 (2003).
641 57. Kyriazis, C. C., Wayne, R. K. & Lohmueller, K. E. High genetic diversity can contribute to
642 extinction in small populations. *bioRxiv* 678524 (2019).

643 58. Robinson, J. A., Brown, C., Kim, B. Y., Lohmueller, K. E. & Wayne, R. K. Purging of strongly
644 deleterious mutations explains long-term persistence and absence of inbreeding depression
645 in island foxes. *Current Biology* **28**, 3487–3494 (2018).
646 59. Bérénos, C., Ellis, P. A., Pilkington, J. G. & Pemberton, J. M. Estimating quantitative genetic
647 parameters in wild populations: a comparison of pedigree and genomic approaches.
648 *Molecular ecology* **23**, 3434–3451 (2014).
649 60. Huisman, J. Pedigree reconstruction from SNP data: parentage assignment, sibship clustering
650 and beyond. *Molecular ecology resources* **17**, 1009–1024 (2017).
651 61. Morrissey, M. B. *et al.* The prediction of adaptive evolution: empirical application of the
652 secondary theorem of selection and comparison to the breeder's equation. *Evolution:*
653 *International Journal of Organic Evolution* **66**, 2399–2410 (2012).
654 62. Aulchenko, Y. S., Ripke, S., Isaacs, A. & Van Duijn, C. M. GenABEL: an R library for genome-
655 wide association analysis. *Bioinformatics* **23**, 1294–1296 (2007).
656 63. Johnston, S. E., Bérénos, C., Slate, J. & Pemberton, J. M. Conserved Genetic Architecture
657 Underlying Individual Recombination Rate Variation in a Wild Population of Soay Sheep (Ovis
658 aries). *Genetics* **203**, 583–598 (2016).
659 64. Jiang, Y. *et al.* The sheep genome illuminates biology of the rumen and lipid metabolism.
660 *Science* **344**, 1168–1173 (2014).
661 65. Purcell, S. *et al.* PLINK: a tool set for whole-genome association and population-based linkage
662 analyses. *The American Journal of Human Genetics* **81**, 559–575 (2007).
663 66. Thompson, E. A. Identity by descent: variation in meiosis, across genomes, and in populations.
664 *Genetics* **194**, 301–326 (2013).
665 67. Bates, D., Mächler, M., Bolker, B. & Walker, S. Fitting linear mixed-effects models using lme4.
666 *Journal of Statistical Software* **67**, (2015).
667 68. Bolker, B. & Robinson, D. *broom.mixed: Tidying Methods for Mixed Models. R package version*
668 *0.2.4.* (2019).
669 69. Rue, H., Martino, S. & Chopin, N. Approximate Bayesian inference for latent Gaussian models
670 by using integrated nested Laplace approximations. *Journal of the royal statistical society:*
671 *Series b (statistical methodology)* **71**, 319–392 (2009).
672 70. Holand, A. M., Steinsland, I., Martino, S. & Jensen, H. Animal models and integrated nested
673 Laplace approximations. *G3: Genes, Genomes, Genetics* **3**, 1241–1251 (2013).
674 71. Gelman, A. & Hill, J. *Data analysis using regression and multilevel/hierarchical models*.
675 (Cambridge university press, 2006).

676 72. Schielzeth, H. Simple means to improve the interpretability of regression coefficients. *Methods*
677 *in Ecology and Evolution* (2010).
678 73. Gao, X., Starmer, J. & Martin, E. R. A multiple testing correction method for genetic association
679 studies using correlated single nucleotide polymorphisms. *Genetic Epidemiology: The Official*
680 *Publication of the International Genetic Epidemiology Society* **32**, 361–369 (2008).
681 74. Holm, S. A simple sequentially rejective multiple test procedure. *Scandinavian journal of*
682 *statistics* 65–70 (1979).
683 75. R Core Team. *R: A language and environment for statistical computing. R Foundation for*
684 *Statistical Computing*. (2019).
685 76. Wickham, H. *ggplot2: elegant graphics for data analysis*. (Springer, 2016).
686